Improving metabolic stability of fluorine-18 labeled verapamil analogs

Raaphorst, Renske M.; Luurtsema, Geert; Schokker, CJ; Attia, KA; Schuit, Robert C.; Elsinga, Philip H.; Lammertsma, Adriaan A.; Windhorst, Albert D.

Published in:
Nuclear Medicine and Biology

DOI:
10.1016/j.nucmedbio.2018.06.009

Nuclear Medicine and Biology 64–65 (2018) 47–56

Contents lists available at ScienceDirect

Nuclear Medicine and Biology

journal homepage: www.elsevier.com/locate/nucmedbio

Improving metabolic stability of fluorine-18 labeled verapamil analogs

Renske M. Raaphorst [a,*], Gert Luurtsema [b], Cindy J. Schokker [a], Khaled A. Attia [a], Robert C. Schuit [a], Philip H. Elsinga [b], Adriaan A. Lammertsma [a], Albert D. Windhorst [a]

[a] Department of Radiology & Nuclear Medicine, VU University Medical Center Amsterdam, the Netherlands
[b] Department of Nuclear Medicine and Molecular Imaging, University of Groningen, University Medical Center Groningen, the Netherlands

ARTICLE INFO

Article history:
Received 24 December 2017
Received in revised form 3 June 2018
Accepted 4 June 2018
Available online xxxx

Keywords:
P-glycoprotein
Positron emission tomography
Deuterium substitution
Deuterium isotope effect
Metabolism
Radiopharmaceuticals

ABSTRACT

Introduction: Fluorine-18 labeled positron emission tomography (PET) tracers were developed to obtain more insight into the function of P-glycoprotein (P-gp) in relation to various conditions. They allow research in facilities without a cyclotron as they can be transported with a half-life of 110 min. As the metabolic stability of previously reported tracers [^{18}F]**1** and [^{18}F]**2** was poor, the purpose of this study was to improve this stability using deuterium substitution, creating verapamil analogs [^{18}F]**1-*d*$_4$**, [^{18}F]**2-*d*$_4$**, [^{18}F]**3-*d*$_3$** and [^{18}F]**3-*d*$_7$**.

Methods: The following deuterium containing tracers were synthesized and evaluated in mice and rats: [^{18}F]**1-*d*$_4$**, [^{18}F]**2-*d*$_4$**, [^{18}F]**3-*d*$_3$** and [^{18}F]**3-*d*$_7$**.

Results: The deuterated analogs [^{18}F]**2-*d*$_4$**, [^{18}F]**3-*d*$_3$** and [^{18}F]**3-*d*$_7$** showed increased metabolic stability compared with their non-deuterated counterparts. The increased metabolic stability of the methyl containing analogs [^{18}F]**3-*d*$_3$** and [^{18}F]**3-*d*$_7$** might be caused by steric hindrance for enzymes.

Conclusion: The striking similar *in vivo* behavior of [^{18}F]**3-*d*$_7$** to that of (*R*)-[^{11}C]verapamil, and its improved metabolic stability compared with the other fluorine-18 labeled tracers synthesized, supports the potential clinical translation of [^{18}F]**3-*d*$_7$** as a PET radiopharmaceutical for P-gp evaluation.

1. Introduction

P-glycoprotein (P-gp) is an ATP dependent efflux transporter, which is i.a. located on the luminal side of the blood-brain barrier [1]. As such, it mediates the transport of structurally diverse compounds from brain to blood, thereby protecting the brain from xenobiotics. P-gp is the most studied ATP-binding cassette (ABC) transporter and it is linked to various neurodegenerative diseases. It has been shown that P-gp function is diminished in Alzheimer's disease, which may accelerate the disease process, as it is associated with decreased clearance of β-amyloid from the brain [2]. On the other hand, several studies have shown increased P-gp function in epilepsy patients, associated with resistance to anti-epileptic drugs [3]. To obtain more insight into the function of P-gp in relation to these and other conditions, positron emission tomography (PET) can be used to investigate the function of P-gp *in vivo* using substrates labeled with positron emitters [4]. (*R*)-[^{11}C]verapamil is a commonly used PET agent for P-gp research, although limited by its relatively short half-life of 20 min. Originally, verapamil was developed and used as a calcium channel blocker [5], but it is also a substrate of P-gp.

Recently, two fluorine-18 labeled positron emission tomography (PET) tracers were developed [6] ([^{18}F]**1** and [^{18}F]**2**, Fig. 1) to image the function of P-gp in the brain, based on the chemical structure of verapamil. Clearly, these tracers could be useful in clinical studies of Alzheimer's disease or epilepsy, where alterations in P-gp function could be detected in a PET scan by increased or decreased brain uptake. Despite their high specificity for P-gp, a disadvantage of these tracers was their poor metabolic stability, as this may compromise quantification, decrease the signal-to-noise ratio and complicate interpretation.

The metabolic pathway of verapamil has been studied in detail [7,8]. Different metabolites were identified and the most important initial metabolites were D-617, norverapamil and D-703. The metabolites and corresponding enzymes are depicted in Fig. 2 [9, 10]. Previous PET studies have shown the formation of corresponding radiolabeled metabolites of (*R*)-[^{11}C]verapamil *in vivo* [11].

It is known that *N*-demethylation of verapamil by cytochrome P450 enzyme, yielding the metabolite norverapamil occurs via the hydrogen atom transfer (HAT) mechanism [12]. Within this reaction, first a hydrogen atom (H) is abstracted creating a radical carbon atom. Next, an alcohol is formed which is cleaved of to form formaldehyde and a secondary amine. Deuterium substitution of the methyl group could be used to slow down this reaction. Cleavage of the covalent bond of carbon (C) with deuterium (D) requires greater energy than cleavage of the bond with hydrogen, due to the higher mass of deuterium,

* Corresponding author at: Department of Radiology & Nuclear Medicine, VU University Medical Center, De Boelelaan 1085C, 1081 HV Amsterdam, the Netherlands.
E-mail address: r.raaphorst@vumc.nl (R.M. Raaphorst).

https://doi.org/10.1016/j.nucmedbio.2018.06.009

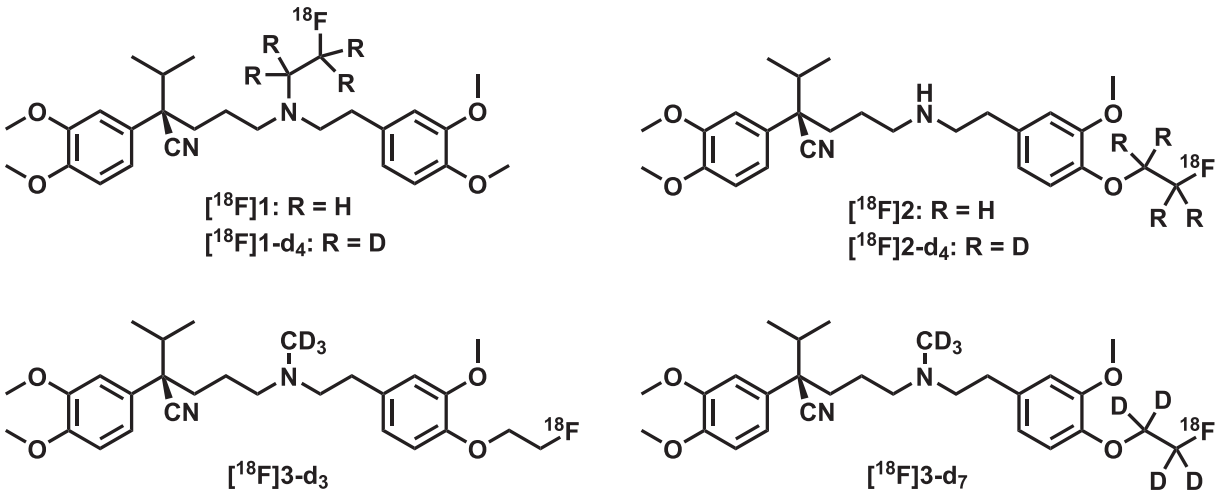

Fig. 1. Chemical structures of deuterated (nor-)verapamil analogs, with measured Log D values.

compared with hydrogen. C—D bonds have a lower vibrational frequency and, thus, lower zero-point energy than an analogous C—H bond. This results in higher activation energy and slower rate for C—D bond cleavage. This rate effect is referred to as the primary deuterium isotope effect [13–15].

The deuterium substitution approach has been used on a number of occasions to fine-tune properties of new pharmaceuticals, primarily related to metabolic stability. The first approval of a deuterium containing drug was provided by the FDA for deutetrabenazine, issued 3rd of April 2017 [16,17]. In addition, in developing new PET tracers, deuterium has occasionally been used to alter properties. The first and most well-known deuterated PET tracer is [^{11}C]L-deprenyl-D_2, which showed slower binding to its target MAO B than the original hydrogen compound resulting in a reduced rate of trapping in (brain) tissue and to improve sensitivity [18]. Multiple deuterated analogs of [^{11}C]- and [^{18}F]-choline showed improved protection against choline oxidation [19,20]. Another example is [^{18}F]deuteroaltanserin, which showed 29% higher ratios of parent tracer to radiometabolites in plasma, compared with [^{18}F]altanserin [21].

In this study, four deuterium substituted analogs were synthesized and evaluated for metabolic stability and *in vivo* behavior. The purpose of this work is to develop a stable fluorine-18 PET tracer for P-gp evaluation, to gain more insight in the metabolic pathways and to investigate which groups are more prone to metabolism.

2. Materials & methods

2.1. General

Chemicals and solvents were purchased from commercial sources Sigma-Aldrich (Zwijndrecht, the Netherlands), Fluorochem (Hadfield Derbyshire, UK), ABCr GmbH (Karlsruhe, Germany) and Biosolve (Valkenswaard, the Netherlands) without further purification unless stated otherwise. Deuterated starting materials ethylene-d_4 glycol, 2-bromoethanol-1,1,2,2-d_4 and Iodomethane-d_3 had an isotopic purity of 98, 98 and ≥99.5 atom % D, respectively. (*R*)-desmethyl-verapamil was kindly donated by Abbott Laboratories (Lake Bluff, IL, USA). Dichloromethane (DCM), 1,2-dichloroethane (DCE), methanol (MeOH) and dimethylformamide (DMF) were dried over 3 Å molecular sieves, for at least 24 h prior to use. Tetrahydrofuran (THF) was first distilled from LiAlH4 and then dried over 3 Å molecular sieves. Thin layer chromatography (TLC) was performed on Merck (Darmstadt, Germany) precoated silica gel 60 F254 plates. Spots were visualized by UV quenching or ninhydrin. Column chromatography was carried out either manually by using silica gel 60 Å (Sigma-Aldrich) or on a Buchi (Flawil, Switzerland) sepacore system (comprising of a C-620 control unit, a C-660 fraction collector, 2 C-601 gradient pumps and a C-640 UV detector) equipped with Buchi sepacore prepacked flash columns. ^{1}H and ^{13}C nuclear magnetic resonance (NMR) spectra were recorded

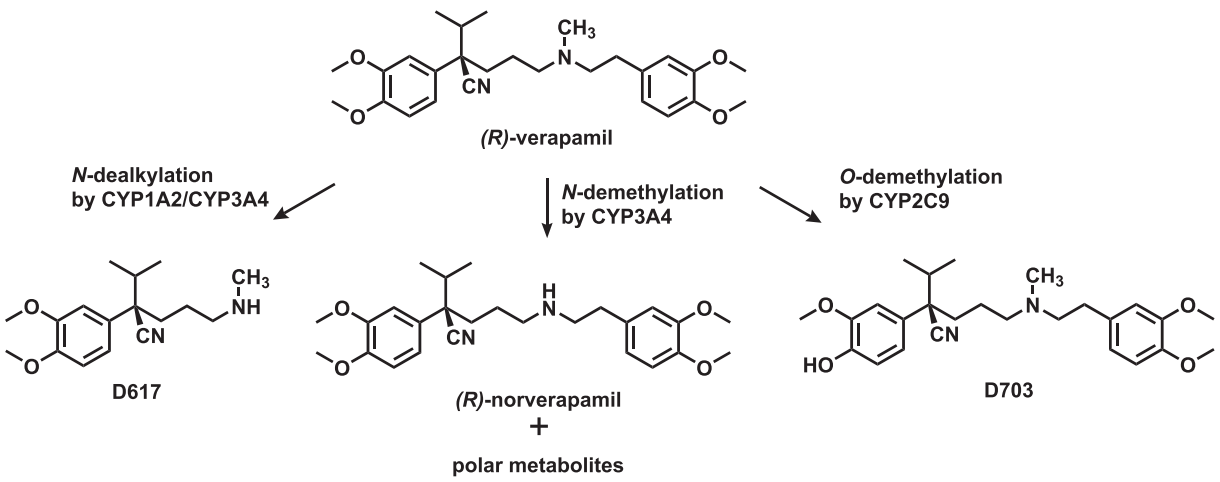

Fig. 2. Metabolic pathway of (*R*) [^{11}C]verapamil as adapted from Luurtsema et al. [11].

on a Bruker (Billerica, USA) Avance 500 (500.23 MHz and 125.78 MHz, respectively) with chemical shifts (δ) reported in ppm relative to the solvent. Electrospray ionization mass spectrometry (ESI-MS) was carried out using a Bruker microTOF-Q instrument in positive ion mode (capillary potential of 4500 V). Solid-phase extraction cartridges (tC18 plus and Alumina N) were purchased from Waters Corp. (Milford, MA, USA).

Semi-preparative HPLC was performed on a Jasco PU-2089 pump station (Easton, MD, USA) equipped with either a Luna C18(2) column (10 μm, 250 mm × 10 mm, Phenomenex, California, USA) using H_2O/MeCN/TFA (60:40:0.2, %v/v/v, method: A) or 5 mM K_3PO_4/MeCN (28:72, %v/v, pH = 10.0, method: B) as eluent, or a Grace Alltima column (10 μm, 250 mm × 22 mm; Hichrom, Theale, Berkshire, UK) using H_2O/MeCN/TFA (50:50:0.1, %v/v/v, method: C) as eluent at a flow rate of 4 mL·min^{-1}, a Jasco UV-2075 Plus UV detector (λ = 254 nm), a custom made radioactivity detector and Jasco ChromNAV CFR software (version 1.14.01) for data acquisition. Quantitative analysis was performed using an HPLC system of Jasco containing a PU-2089 pump station equipped with a Grace Alltima C18 column (5 μm, 250 mm × 4.6 mm) using H_2O/MeCN/DIPA (40:60:0.1, %v/v/v, method: D), H_2O/MeCN/TFA (50:50:0.1, %v/v/v, method: E) or H_2O/MeCN/TFA (60:40:0.1, %v/v/v, method: F) as eluent at a flow rate of 1 mL·min^{-1}, with a Jasco UV-2075 UV detector (λ = 232 nm) and a Sodium Iodide (NaI) radioactivity detector (Raytest, Straubenhardt, Germany). Chromatograms were acquired using Raytest GINA Star software (version 5.01).

Metabolite analysis was performed on Dionex (Sunnyvale, CA, USA) UltiMate 3000 HPLC equipment with Chromeleon software (version 6.8). A LUNA C8 (5 μm, 250 mm × 10 mm, Phenomenex (Torrance, CA, USA)) column was used (method G) using 5 mM NH_4OAc/MeCN (1:1, %v/v, pH = 4.2) as eluent at a flow rate of 3.5 mL·min^{-1}.

2.1.1. 2-Bromoethyl-1,1,2,2-d_4 4-methylbenzenesulfonate (6)

4-Methylbenzene-1-sulfonyl chloride (924 mg, 4.85 mmol) was dissolved in DCM (3 mL) at 0 °C. Et_3N (0.675 mL, 4.85 mmol) and 2-Bromoethanol-1,1,2,2-d_4 (0.275 mL, 3.88 mmol) were added drop-wise to the reaction mixture. The mixture was stirred for 1 h at 0 °C. The reaction mixture was brought to room temperature, washed with water and brine and dried over Na_2SO_4. The solvent was evaporated in vacuo, and the residue was purified by flash column chromatography (10% EtOAc in hexane), obtaining the 2-bromoethanol-1,1,2,2-d_4-methylbenzene-1-sulfonyl product (0.988 mg, 3.53 mmol, 91% yield) as colorless oil. ^{1}H NMR ($CDCl_3$) δ 7.83 [2H, d, J = 8.3 Hz, SO_2-CH_{AR}], 7.38 [2H, d, J = 8.0 Hz, CH_3-CH_{AR}], 2.48 [3H, s, TsCH_3] ^{13}C NMR ($CDCl_3$) δ 145.21, 132.67, 129.95, 127.95, 21.65 ESI-HRMS: calculated for $C_9H_7d_4BrO_3S$: 281.9863, 282.9936 $[M + H]^+$ and 304.9749 $[M + Na]^+$ found.

2.1.2. Ethane-1,2-diyl-d_4 bis(4-methylbenzenesulfonate) (7)

Ethylene-d_4 glycol (0.19 mL, 3.40 mmol) was dissolved in DCM (5 mL) and brought to 0 °C, and then 4-methylbenzene-1-sulfonyl chloride (2.19 g, 11.5 mmol) and triethylamine (1.58 mL, 11.3 mmol) were added. The reaction mixture was stirred starting from 0 °C to room temperature, overnight. The reaction was quenched with water, and crude product was extracted with DCM, washed with water and brine, and dried over Na_2SO_4 after which the solvent was evaporated in vacuo. The brown solid was purified by flash column chromatography (20–50% EtOAc in hexane) resulting in a white powder (1.33 g, 3.55 mmol, quantitative yield). ^{1}H NMR ($CDCl_3$) δ 7.73 [4H, d, J = 8.3 Hz, SO_2-CH_{AR}], 7.33 [4H, d, J = 8.1 Hz CH_3-CH_{AR}], 2.46 [6H, s, CH_3]. ^{13}C NMR ($CDCl_3$) δ (ppm) 145, 132, 130, 128, 22. ESI-HRMS: calculated for $C_{16}H_{14}d_4O_6S_2$: 374.0796, 375.0900 $[M + H]^+$ and 397.0728 $[M + Na]^+$ found.

2.1.3. 2-(4-(2-((tert-Butoxycarbonyl)amino)ethyl)-2-methoxyphenoxy) ethyl-1,1,2,2-d_4 4-methylbenzenesulfonate (9)

tert-Butyl 4-hydroxy-3-methoxyphenethylcarbamate (417 mg, 1.56 mmol) was dissolved in DMF (50 mL) and cesium carbonate (1.02 g, 3.12 mmol) and d_4-ethane-1,2-diyl bis(4-methylbenzenesulfonate) (1.17 g, 3.12 mmol) were added. The yellow clear mixture was stirred at room temperature and after 4 h it turned into a green cloudy mixture. The reaction was quenched with water. The crude product was extracted twice with EtOAc, washed with brine, dried over Na_2SO_4 and the solvent was evaporated in vacuo. The yellow oil was purified by flash column chromatography (20% EtOAc in hexane) resulting in a white powder (754 mg, 1.60 mmol, quantitative yield). ^{1}H NMR ($CDCl_3$) δ 7.82 [2H, d, J = 8.4 Hz, SO_2-CH_{AR}], 7.33 [2H, d, J = 8.4 Hz CH_3-CH_{AR}], 6.77–6.65 [3H, m, CH_{AR}], 4.55 [1H, br s, NH], 3.82 [3H, s, OCH_3], 3.34 [2H, q, J = 6.5, NHCH_2CH_2], 2.73 [2H, t, J = 7.1, NHCH_2CH_2], 2.45 [3H, s, TsCH_3], 1.44 [9H, s, Boc]. ^{13}C NMR ($CDCl_3$) δ 155.82, 149.88, 146.01, 144.83, 133.29, 132.87, 129.80, 127.99, 120.78, 115.32, 112.80, 79.22, 55.88, 41.81, 35.78, 28.39, 21.64. ESI-HRMS: calculated for $C_{23}H_{27}d_4NO_7S$: 469.2072; 470.2179 $[M + H]^+$ and 492.2010 $[M + Na]^+$ found.

2.1.4. 2-(4-(2-Aminoethyl)-2-methoxyphenoxy)ethyl-1,1,2,2-d_4 4-methylbenzenesulfonate (10)

2-(4-(2-((*tert*-Butoxycarbonyl)amino)ethyl)-2-methoxyphenoxy) ethyl-1,1,2,2-d_4 4-methylbenzenesulfonate (61 mg, 0.13 mmol) was dissolved in DCM (5 mL) and TFA (5 mL) was added. The reaction mixture was stirred at room temperature for 1 h after which it was diluted with DCM and the solvent was evaporated in vacuo. The light brown oil was purified by flash column chromatography (4–10% MeOH in DCM) to obtain the desired white crystals (52 mg, 0.14 mmol, quantitative yield). ^{1}H NMR (MeOD) δ 7.80 [2H, d, J = 8.1 Hz, SO_2-CH_{AR}], 7.42 [2H, d, J = 8.1 Hz CH_3-CH_{AR}], 6.88–6.73 [3H, m, CH_{AR}], 3.82 [3H, s, OCH_3], 3.15 [2H, q, J = 7.8 Hz, NHCH_2CH_2], 2.88 [2H, t, J = 7.8 Hz, NHCH_2CH_2] , 2.44 [3H, s, TsCH_3]. ^{13}C NMR (MeOD) δ 151.68, 148.28, 146.64, 134.38, 132.09, 131.18, 129.16, 122.23, 116.70, 114.30, 56.64, 42.12, 34.28, 21.74. ESI-HRMS: calculated for $C_{18}H_{19}d_4NO_5S$: 369.1548; 370.1608 $[M + H]^+$ found.

2.1.5. (R)-2-(4-(2-((tert-butoxycarbonyl)(4-cyano-4-(3,4-dimethoxyphenyl)-5-methylhexyl)amino)ethyl)-2-methoxyphenoxy)ethyl-1,1,2,2-d_4 4-methylbenzenesulfonate (17)

Na_2SO_4 (55 mg, 0.39 mmol) and (*R*)-2-(3,4-dimethoxyphenyl)-2-isopropyl-5-oxopentanenitrile (151 mg, 0.547 mmol) in 1.7 mL DCE were added to a solution of 2-(4-(2-aminoethyl)-2-methoxyphenoxy) ethyl-1,1,2,2-d_4 4-methylbenzenesulfonate [6] (223 mg, 0.604 mmol) in 1.7 mL DCE. The reaction mixture was stirred at room temperature overnight under N_2. Sodium triacetoxyhydroborate (132 mg, 0.623 mmol) was added to the mixture and stirred for 1.5 h at room temperature. The reaction was quenched with 1 M $NaHCO_3$, extracted with EtOAc (10 mL), washed with water (2×) and brine, organic layers were dried over Na_2SO_4, and used as such in the next step. Di-*tert*-butyl dicarbonate (185 mg, 0.848 mmol) and triethylamine (120 μL, 0.866 mmol) were added to diluted crude product and stirred at room temperature for 1.5 h. The reaction mixture was diluted with EtOAc, washed with water and brine, dried over Na_2SO_4, and solvent was removed in vacuo. The crude mixture was purified by flash column chromatography (30–50% EtOAc/Hex) to obtain the purified product as colorless oil (37 mg, 0.051 mmol, 13% yield). ^{1}H NMR ($CDCl_3$) δ 7.82 [2H, d, J = 8.2 Hz, SO_2-CH_{AR}], 7.33 [2H, d, J = 8.2 Hz, CH_3-CH_{AR}], 6.89–6.62 [6H, m, CH_{AR}], 3.88 [3H, s, OCH_3], 3.87 [3H, s, OCH_3], 3.80 [3H, s, OCH_3], 3.29–2.99 [4H, m, CH_2NCH_2], 2.67 [2H, br s, NCH_2CH_2Ar], 2.44 [3H, s, TsCH_3], 2.06 [2H, m, CH_2CH_2CH_2], 1.80–1.55 [3H, m, CH(CH_3)$_2$ and CCH_2], 1.43 [9H, m, Boc], 1.17 and 0.78 [3H each, d, J = 6.3 Hz, CH(CH_3)$_2$]. ^{13}C NMR ($CDCl_3$) δ 149.69, 148.96, 148.43, 148.21, 145.83, 144.83, 133.40, 132.75, 130.36, 129.79, 127.97, 120.74, 118.65, 115.14, 112.76, 110.97, 109.26, 79.38, 55.90, 55.83, 55.82, 49.08, 48.67, 47.27, 37.87, 35.14, 34.79, 28.36, 24.62, 21.64, 18.90, 18.51. ESI-HRMS: calculated for $C_{39}H_{48}d_4N_2O_9S$: 728.3645, 729.4104 $[M + H]^+$ and 751.3935 $[M + Na]^+$ found.

2.1.6. tert-Butyl (4-(2-fluoroethoxy-1,1,2,2-d_4)-3-methoxyphenethyl) carbamate (11)

2-(4-(2-((*tert*-Butoxycarbonyl)amino)ethyl)-2-methoxyphenoxy) ethyl-d_4 4-methylbenzenesulfonate (471 mg, 1.00 mmol) and TBAF (446 mg, 1.71 mmol) were co-evaporated three times with dry acetonitrile to remove any water. Compounds were dissolved in acetonitrile (5 mL) and added to a closed reaction vial. The reaction mixture was stirred at 85 °C in heatblock for 4 h. Solvent was evaporated and crude mixture was purified by flash column chromatography (10–25% EtOAc in hexane) to obtain the desired clear oil (254 mg, 0.800 mmol, 80%). ^{1}H NMR ($CDCl_3$) δ 6.88–6.71 [3H, m, CH_{AR}], 4.55 [1H, br s, NH_2], 3.87 [3H, s, OCH_3], 3.36 [2H, q, J = 6.6 Hz, $NHCH_2CH_2$], 2.75 [2H, t, J = 7.0, $NHCH_2CH_2$], 1.44 [9H, s, Boc]. ^{13}C NMR ($CDCl_3$) δ 155.71, 149.52, 146.15, 132.70, 120.51, 114.34, 112.44, 78.85, 55.61, 41.65, 35.54, 28.17. ESI-HRMS: calculated for $C_{16}H_{20}d_4FNO_4$: 317.1940, 340.1856 [M + Na]$^+$ found.

2.1.7. 2-(4-(2-Fluoroethoxy-1,1,2,2-d_4)-3-methoxyphenyl)ethan-1-amine (12)

tert-Butyl 4-(2-fluoroethoxy)-3-methoxyphenethyl-d_4-carbamate (253 mg, 0,797 mmol) was dissolved in DCM (12 mL), TFA (12 mL) was added and the mixture was stirred at room temperature for 1 h. Reaction mixture was diluted with DCM and solvent was evaporated under vacuo. Crude mixture was purified by flash column chromatography (3–5% MeOH in DCM) to obtain the desired product as a white solid (174 mg, 0.800 mmol, quantitative yield). ^{1}H NMR (MeOD) δ 6.95–6.78 [3H, m, CH_{AR}], 3.85 [3H, s, OCH_3], 3.16 [2H, t, J = 7.6 Hz, $NHCH_2$], 2.90 [2H, t, J = 8.0 Hz, $NHCH_2CH_2$]. ^{13}C NMR ($CDCl_3$) δ (ppm) 151.57, 148.78, 131.72, 122.32, 116.09, 114.20, 56.61, 42.15, 34.30. ESI-HRMS: calculated for $C_{11}H_{12}d_4FNO_2$: 217.1416, 218.1559 [M + H]$^+$ found.

2.1.8. (R)-2-(3,4-dimethoxyphenyl)-5-((4-(2-fluoroethoxy-1,1,2,2-d_4)-3-methoxyphenethyl)amino)-2-isopropylpentanenitrile (18)

2-(4-(2-Fluoroethoxy)-3-methoxyphenyl)ethane-d_4-amine (174 mg, 0.800 mmol) was dissolved in dry MeOH (3 mL) and Na_2SO_4 (600 mg, 4.2 mmol) was added. (*R*)-2-(3,4-dimethoxyphenyl)-2-isopropyl-5-oxopentanenitrile (147 mg, 0.534 mmol) was dissolved in dry MeOH (1.4 mL), added to the mixture, which was stirred at room temperature overnight under nitrogen. Sodium triacetoxyhydroborate (170 mg, 0.800 mmol) was added and stirred at room temperature for 2 h. The reaction was quenched with 1 M $NaHCO_3$ and extracted with EtOAc, washed with H_2O and brine, dried over Na_2SO_4 and the solvent was evaporated in vacuo. The crude oil was purified by column chromatography (2–7% MeOH in DCM) to obtain the desired product (30 mg, 0.063 mmol, 12% yield). ^{1}H NMR ($CDCl_3$) δ 6.96–6.68 [6H, m, CH_{AR}], 3.89 [3H, s, OCH_3], 3.87 [3H, s, OCH_3], 3.84 [3H, s, OCH_3], 2.89 [4H, m, $CH_2NCH_2CH_2$], 2.75 [2H, t, J = 6.9 Hz, NCH_2CH_2], 2.20 and 1.93 [1H each, dt, J = 12.0 and 4.5, CCH_2], 2.07 [1H, sept, J = 6.8 Hz, $CH(CH_3)_2$], 1.67 and 1.32 [1H each, m, $CH_2CH_2CH_2$], 1.18 and 0.79 [3H each, d, J = 6.6, $CH(CH_3)_2$]. ^{13}C NMR ($CDCl_3$) δ 149.85, 149.05, 148.35, 146.60, 131.87, 129.99, 121.14, 120.57, 118.63, 114.59, 112.58, 111.06, 109.37, 55.97, 55.92, 55.81, 49.53, 47.97, 37.87, 35.02, 33.78, 23.91, 18.85, 18.52. ESI-HRMS: calculated for $C_{27}H_{33}D_4FN_2O_4$: 476.2988, 477.3542 [M + H]$^+$ found.

2.1.9. (R)-2-(4-(2-((4-cyano-4-(3,4-dimethoxyphenyl)-5-methylhexyl)(methyl-d_3)amino)ethyl)-2-methoxyphenoxy)ethyl-1,1,2,2-d_4 4-methylbenzenesulfonate (16)

2-(4-(2-Aminoethyl)-2-methoxyphenoxy)ethyl 4-methylbenzenesulfonate-d_4 (219 mg, 0.592 mmol) and (*R*)-2-(3,4-dimethoxyphenyl)-2-isopropyl-5-oxopentanenitrile (110 mg, 0.403 mmol) were stirred together with Na_2SO_4 (1.5 g) in DCE (3 mL) under nitrogen overnight. The reaction mixture turned light yellow and sodium triacetoxyhydroborate (137 mg, 0.645 mmol) was added and the resulting mixture was stirred at room temperature for 2 h. The reaction was quenched with 1 M $NaHCO_3$, extracted with EtOAc, washed with water and brine, organic layers were dried over Na_2SO_4, and used as such in next step. Iodomethane-d_3 (45.0 μL, 0.723 mmol) and D*i*PEA (200 μL, 1.15 mmol) were added to the reaction mixture and stirred overnight at room temperature. The reaction mixture was diluted with EtOAc, washed with water and brine, dried over Na_2SO_4 and solvent was removed in vacuo. The crude mixture was purified by flash column chromatography (2% MeOH in DCM) and HPLC (method C) to obtain the product as a white solid (5 mg, 0.007 mmol, 2% yield). ^{1}H NMR (MeOD) δ 7.81 [2H, d, J = 8.0 Hz, SO_2-CH_{AR}], 7.42 [2H, d, J = 8.2 Hz, CH_3-CH_{AR}], 7.04–6.67 [6H, m, CH_{AR}], 3.84 [3H, s, OCH_3], 3.82 [3H, s, OCH_3], 3.80 [3H, s, OCH_3], 3.15–2.88 [4H, m, CH_2NCH_2], 2.45 [3H, s, $TsCH_3$], 2.22–2.03 [3H, m $CH(CH_3)_2$ and CCH_2], 1.75 and 1.38 [1H each, br s, $CH_2CH_2CH_2$], 1.31 [2H, br s, NCH_2CH_2Ar], 1.22 and 0.79 [3H each, d, J = 6.6 Hz, $CH(CH_3)_2$]. ^{13}C NMR ($CDCl_3$) δ 151.78, 151.16, 150.51, 148.49, 146.65, 134.48, 131.46, 131.26, 131.20, 129.21, 122.21, 122.16, 120.56, 116.64, 114.27, 112.98, 110.94, 56.79, 56.70, 56.58, 56.51, 38.88, 35.48, 33.24, 30.88, 23.91, 22.34, 21.76, 19.50, 19.03. ESI-HRMS: calculated for $C_{35}H_{39}d_7N_2O_7S$: 645.3465, 646.3498 [M + H]$^+$ found.

2.1.10. (R)-2-(4-(2-((4-cyano-4-(3,4-dimethoxyphenyl)-5-methylhexyl)(methyl-d_3)amino)ethyl)-2-methoxyphenoxy)ethyl 4-methylbenzenesulfonate (19)

2-(4-(2-Aminoethyl)-2-methoxyphenoxy)ethyl 4-methylbenzenesulfonate (341 mg, 0.935 mmol) and (*R*)-2-(3,4-dimethoxyphenyl)-2-isopropyl-5-oxopentanenitrile (177 mg, 0.644 mmol) were stirred together with Na_2SO_4 (1.5 g) in DCE (5 mL) under nitrogen overnight. The reaction mixture turned light yellow and sodium triacetoxyhydroborate (206 mg, 0.971 mmol) was added and this mixture was stirred at room temperature for 1.5 h. The reaction was quenched with 1 M $NaHCO_3$, extracted with EtOAc, washed with water and brine, after which organic layers were dried over Na_2SO_4 and used as such in the next step. Iodomethane-d_3 (65.0 μL, 1.04 mmol) and D*i*PEA (290 μL, 1.66 mmol) were added to the reaction mixture and stirred overnight at room temperature. The reaction mixture was diluted with EtOAc, washed with water and brine, dried over Na_2SO_4 and solvent was removed in vacuo. The crude mixture was purified by flash column chromatography (2% MeOH in DCM) and HPLC (method C) to obtain the product as a white solid (12 mg, 0.019 mmol, 3.0% yield). ^{1}H NMR ($CDCl_3$) δ 7.81 [2H, d, J = 8.2 Hz, SO_2-CH_{AR}], 7.42 [2H, d, J = 8.2 Hz, CH_3-CH_{AR}], 7.04–6.67 [6H, m, CH_{AR}], 4.32 [2H, t, J = 4.4 Hz, CH_2CH_2OTs], 4.15 [2H, t, J = 4.4 Hz, CH_2CH_2OTs], 3.84 [3H, s, OCH_3], 3.82 [3H, s, OCH_3], 3.80 [3H, s, OCH_3], 3.16–2.89 [4H, m, CH_2NCH_2], 2.45 [3H, s, $TsCH_3$], 2.22–2.04 [3H, m, $CH(CH_3)_2$ and CCH_2], 1.75 and 1.37 [1H each, br s, $CH_2CH_2CH_2$], 1.31 [2H, br s, NCH_2CH_2Ar], 1.22 and 0.79 [3H each, d, J = 6.6 Hz, $CH(CH_3)_2$] . ^{13}C NMR ($CDCl_3$) δ 151.76, 151.14, 150.49, 148.46, 146.66, 134.45, 131.45, 131.32, 131.20, 129.21, 122.20, 122.16, 120.56, 116.67, 114.27, 112.96, 110.93, 70.35, 68.61, 56.79, 56.70, 56.58, 56.50, 38.88, 35.48, 33.24, 30.87, 23.90, 22.38, 21.76, 19.50, 19.03. ESI-HRMS: calculated for $C_{35}H_{43}d_3N_2O_7S$: 641.3214, 642.3302 [M + H]$^+$ found.

2.1.11. (R)-2-(3,4-dimethoxyphenyl)-5-((4-(2-fluoroethoxy)-3-methoxyphenethyl)(methyl-d_3)amino)-2-isopropylpentanenitrile (20)

(*R*)-2-(3,4-dimethoxyphenyl)-2-isopropyl-5-oxopentanenitrile (147 mg, 0.534 mmol) was dissolved in 1.4 mL MeOH and added to a suspension of 2-(4-(2-fluoroethoxy)-3-methoxyphenyl)ethane-d_4-amine (174 mg, 0.801 mmol) and Na_2SO_4 (613 mg) in 3 mL dry MeOH. The reaction mixture was stirred overnight at room temperature under nitrogen. Sodium triacetoxyhydroborate (170 mg, 0.801 mmol) was added and the mixture was stirred again at room temperature for 2 h. The reaction was quenched with 1 M $NaHCO_3$ and extracted with EtOAc, washed with water and brine, dried over Na2SO4 and solvent was removed in vacuo to an oil. The crude mixture was purified by flash column chromatography (2–7% MeOH in DCM) to obtain the desired product as a light brown oil (30 mg, 0.063 mmol, 12% yield). ^{1}H NMR ($CDCl_3$) δ 6.94–6.66 [6H, m, CH_{AR}], 4.77 [2H, dt, J = 47.4 and 4.2 Hz, CH_2CH_2F], 4.25 [2H, dt, J = 27.8 and 4.3 Hz, CH_2CH_2F], 3.89

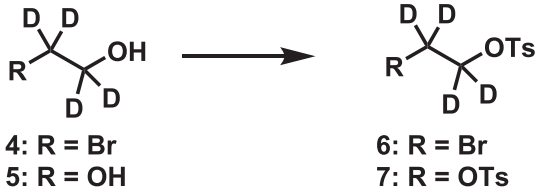

Scheme 1. Reagents and conditions: TsCl, Et_3N, DCM, 0 °C, 1 h (**4** to **6**) or 16 h (**5** to **7**).

[3H, s, OCH_3], 3.88 [3H, s, OCH_3], 3.86 [3H, s, OCH_3], 2.71–2.48 [4H, m, $CH_2NCH_2CH_2$], 2.38 [2H, m, NCH_2CH_2], 2.13 and 1.84 [1H each, dt, J = 12.0 and 4.2, CCH_2], 2.06 [1H, sept, J = 6.7 Hz, $CH(CH_3)_2$], 1.56 and 1.16 [1H each, m, $CH_2CH_2CH_2$] 1.20 and 0.81 [3H each, d, J = 6.8, $CH(CH_3)_2$]. ^{13}C NMR ($CDCl_3$) δ 149.65, 148.91, 148.17, 146.09, 134.25, 130.57, 121.43, 120.54, 118.60, 114.55, 112.67, 110.97, 109.40, 82.69, 81.33, 68.72, 68.56, 59.27, 56.78, 55.93, 55.92, 55.84, 37.91, 35.56, 33.14, 23.27, 18.95, 18.58. ESI-HRMS: calculated for $C_{28}H_{36}d_3FN_2O_4$: 489.3082; 490.3212 $[M + H]^+$ found.

2.2. Radiochemistry

2.2.1. (R)-5-((3,4-dimethoxyphenethyl)(2-[^{18}F]fluoroethyl-1,1,2,2-d_4)amino)-2-(3,4-dimethoxyphenyl)-2-isopropylpentanenitrile ([^{18}F]**1-d_4**)

[^{18}F]F^- was produced by the $^{18}O(p,n)^{18}F$ nuclear reaction using an IBA (Louvain-la-Neuve, Belgium) Cyclone 18/9 cyclotron. Radioactivity levels were measured using a Veenstra (Joure, The Netherlands) VDC-405 dose calibrator. Radiochemistry was carried out in homemade, remotely controlled synthesis units [22]. After irradiation, [^{18}F]fluoride was trapped on a PS-HCO_3 column and eluted using 1 mL MeCN/H_2O (9:1, %v/v) containing Kryptofix 2.2.2 (3 mg, 35 μmol) and K_2CO_3 (2 mg, 14 μmol) into a screw cap reaction vial. The [^{18}F]K_{222}/KF/K_2CO_3 complex was dried at 90 °C under a Helium flow of 50 mL·min^{-1} and reduced pressure for 6 min. 0.5 mL MeCN was added and the complex was dried for 3 min resulting in a white tarnish on the bottom of the vial. Precursor **6** (10 mg, 36 μmol) was dissolved in 0.5 mL DMF and added to the vial with the dried complex. This reaction mixture was heated to 90 °C. After 10 min, the formed volatile intermediate 1-bromo-2-[^{18}F]fluoroethane-d_4 was distilled at 100 °C through a preheated silver triflate column at 200 °C, resulting in [^{18}F]fluoroethyl-d_4-triflate, which was bubbled to the second reaction vial containing a reaction mixture with (*R*)-desmethyl-norverapamil (1.5 mg, 3.4 μmol), K_2CO_3 (1.5 mg, 11 μmol) and a stirring bar in 0.5 mL ACN at 0 °C (Scheme 3). After distillation, the reaction was stirred for 15 min at 120 °C, quenched with 1 mL of water and purified by semi-preparative HPLC (method B). The product eluted at 8 min, and the product fraction was collected for 1.5 min, which was diluted with 40 mL of water. The mixture was passed through a Sep-Pak Plus tC18 cartridge and subsequently rinsed with 20 mL water. The product was eluted from the Sep-Pak Plus tC18 cartridge with 1 mL ethanol (96%) and was diluted with a solution of 7.11 mM NaH_2PO_4 in 0.9% NaCl (*w*/*v* in water), pH 5.2 resulting in a final solution with 5% ethanol. The radiochemical purity was determined by analytical HPLC (method D) to be >99% and the molar radioactivity was 201 ± 88 GBq·μmol^{-1} (n = 3). The radiochemical yield was 2.64 ± 2.26%, decay corrected (DC) (n = 7) calculated from start of synthesis.

2.2.2. (R)-2-(3,4-dimethoxyphenyl)-5-((4-(2-[^{18}F]fluoroethoxy-1,1,2,2-d_4)-3-methoxyphenethyl)amino)-2-isopropylpentanenitrile ([^{18}F]**2-d_4**)

Precursor **17** (1.0 mg, 1.3 μmol) was dissolved in 0.5 mL MeCN, added to the dried [^{18}F]K_{222}/KF/K_2CO_3 complex, and heated at 90 °C for 15 min. The reaction mixture was cooled down to room temperature and TFA (0.2 mL, 2.7 μmol) was added. After 10 min, the reaction was quenched with 0.9 mL of 2.5 M NaOH and purified by semi-preparative HPLC (method A). The product eluted at 15 min, and the product fraction of 1.5 min was diluted with 40 mL of water. This mixture was passed through the Sep-Pak Plus tC18 cartridge and subsequently rinsed with 20 mL water. The product was eluted with 1 mL ethanol (96%) and diluted with a solution of 7.11 mM NaH_2PO_4 in 0.9% NaCl (*w*/*v* in water), pH 5.2 resulting in a final solution with 5% ethanol, with a radiochemical purity of >99% determined by analytical HPLC (method F). The molar radioactivity was 104 ± 48 GBq·μmol^{-1} (n = 2) and the radiochemical yield 6.1 ± 2.6% DC (n = 3) calculated from start of synthesis.

2.2.3. (R)-2-(3,4-dimethoxyphenyl)-5-((4-(2-[^{18}F]fluoroethoxy)-3-methoxyphenethyl)(methyl-d_3)amino)-2-isopropylpentanenitrile ([^{18}F]**3-d_3**)

Precursor **19** (0.5 mg, 0.8 μmol) was dissolved in 0.5 mL MeCN, added to the dried [^{18}F]K_{222}/KF/K_2CO_3 complex and heated at 90 °C for 15 min. The reaction mixture was passed through a Sep-Pak Alumina N light cartridge and rinsed with 1.5 mL MeCN and 1 mL air. The eluate was diluted with 1.5 mL water and purified by semi-preparative HPLC (method A). The product eluted at 15 min, and the product fraction of 1.5 min was diluted with 40 mL of water. The mixture was passed through the Sep-Pak Plus tC18 cartridge and subsequently rinsed with 20 mL water. The product was eluted with 1 mL ethanol (96%) and diluted with a solution of 7.11 mM NaH_2PO_4 in 0.9% NaCl (*w*/*v* in water), pH 5.2 resulting in a final solution with 5% ethanol, with a radiochemical purity of >99.5% determined by analytical HPLC (method E). The molar radioactivity was 125 GBq·μmol^{-1} (n = 1) and the radiochemical yield was 2.74 ± 0.71% DC from start of synthesis (n = 3).

2.2.4. (R)-2-(3,4-dimethoxyphenyl)-5-((4-(2-[^{18}F]fluoroethoxy-1,1,2,2-d_4)-3-methoxyphenethyl)(methyl-d_3)amino)-2-isopropylpentanenitrile ([^{18}F]**3-d_7**)

[^{18}F]**3-d_7** was prepared using an identical procedure as for [^{18}F]**3-d_3**, starting with precursor **16** (0.5 mg, 0.8 μmol). The radiochemical purity was >99.5% determined by analytical HPLC (method E). The molar radioactivity was 91.3 ± 25.5 GBq/μmol (n = 5) and the radiochemical yield was 4.90 ± 3.86% DC from start of synthesis (n = 5).

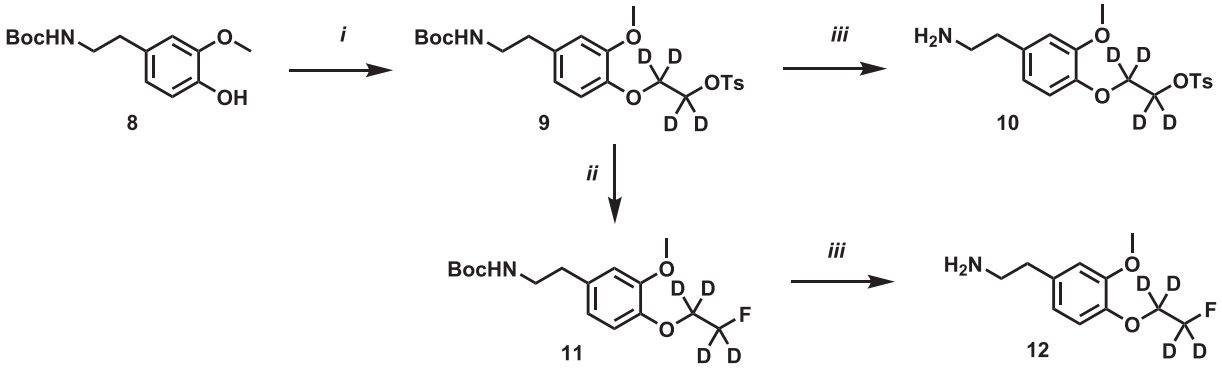

Scheme 2. Reagents and conditions: i) **7**, Cs_2CO_3, DMF, r.t., 4 h; ii) TBAF, MeCN, 85 °C, 4 h; iii) TFA, DCM, r.t., 1 h.

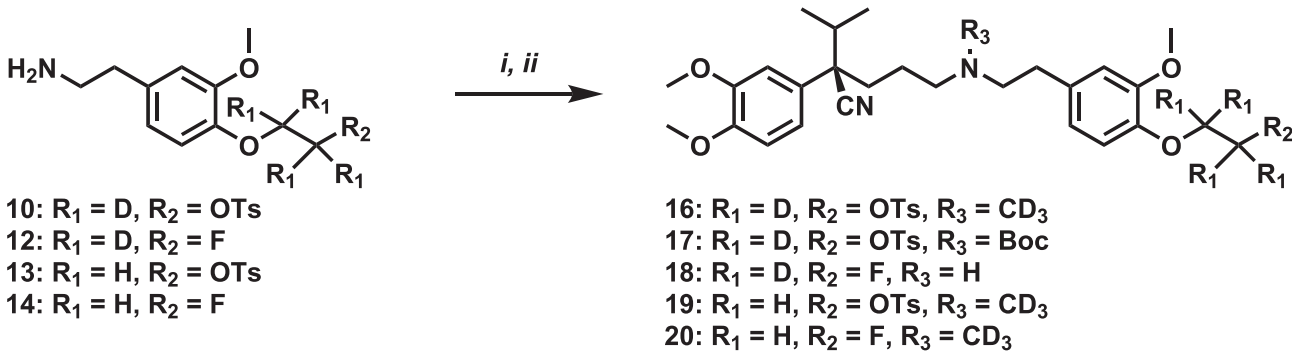

Scheme 3. Reagents and conditions: i) (*R*) aldehyde **15** [6], $NaBH(OAc)_3$, Na_2SO_4, DCE, r.t., 18 h. For **12** directly to **18**. Next step for **10**, **13** and **14** to form **16**, **19** and **20**, respectively: ii) CD_3I, *Di*PEA, r.t., 18 h. Only for **10** to form **17**: Boc_2O, Et_3N, r.t., 1.5 h.

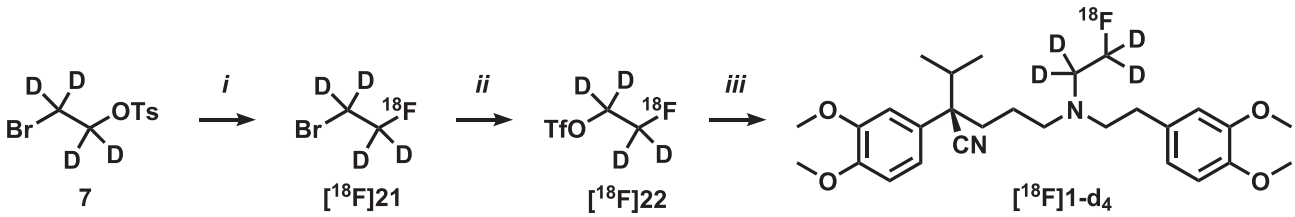

Scheme 4. Reagents and conditions: i) $^{18}F/K_{2.2.2}/K^+$, DMF, 90 °C, 15 min; ii) AgOTf, 200 °C, 15 min; iii) norverapamil, K_2CO_3, MeCN, 120 °C, 15 min.

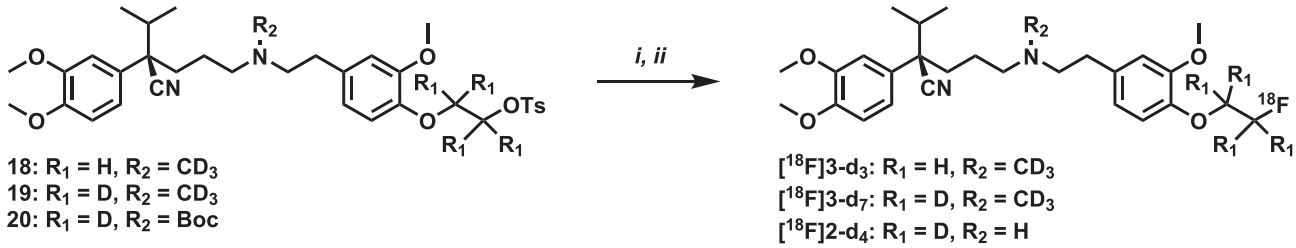

Scheme 5. Reagents and conditions: i) $^{18}F/K_{2.2.2}/K^+$, MeCN, 90 °C, 15 min; only for [^{18}F]**2 *d*$_4$**: ii) TFA, r.t., 10 min.

2.3. General procedure for log $D_{7.4}$ measurements

The distribution of the tracers between equal volumes of 0.2 M phosphate buffer (pH = 7.4) and 1-octanol was measured in triplicate at room temperature. 1 mL of a 1–5 MBq·mL^{-1} solution of the fluorine-18 labeled tracers in 0.2 M phosphate buffer (pH = 7.4) was vigorously mixed with 1 mL of 1-octanol for 1 min at room temperature using a vortex. After 30 min, five samples of 100 μL were taken from both layers, avoiding cross-contamination. To determine recovery, 5 samples of 100 mL were taken from the 1–5 MBq·mL^{-1} solution. All samples were counted for radioactivity. The Log $D_{oct,7.4}$ value was calculated according to Log $D_{oct,7.4} = {}^{10}\mathrm{Log}(A_{oct}/A_{buffer})$, where A_{oct} and A_{buffer} represent average radioactivity of 5 1-octanol and 5 buffer samples, respectively [23].

2.4. Animals

Healthy male Wistar rats were obtained from Harlan Netherlands B.V. (Horst, the Netherlands) and male FVB wild-type mice and *Mdr1a/b*$^{(-/-)}$ mice developed from the FVB line were purchased from Taconic (Hudson, USA). All animals were housed in groups of four to six per cage under standard conditions (24 °C, 60% relative humidity, 12-h light/dark cycles) and provided with water and food (Teklad Global 16% Protein Rodent Diet, Harlan, Madison, WI, USA) ad libitum. All animal experiments were performed in compliance with Dutch laws on animal experimentation ('Wet op de proefdieren', Stb 1985, 336) and after approval by the local animal ethics committee.

2.5. Metabolite analysis

Under isoflurane anesthesia, healthy Wistar rats (198–286 g) received tail vein injection of 36.8 ± 5.7, 30.2 ± 5.0, 24.4 ± 5.2 or 38.6 ± 6.1 MBq of [^{18}F]**1-*d*$_4$**, [^{18}F]**2-*d*$_4$**, [^{18}F]**3-*d*$_3$** or [^{18}F]**3-*d*$_7$**, respectively, in 0.2–0.4 mL. After injection, rats were conscious for the allowed time (except for the animals of the 5 min time point, which were left unconscious for the whole time) and sacrificed under isoflurane anesthesia at 5, 15 or 60 min ($n = 3$ for each time point). Blood samples were collected via a heart puncture, and the brain was removed from the skull and cut in half. Blood was collected in a heparin tube and centrifuged for 5 min at 4000 rpm (Hettich universal 16, Depex B.V., the Netherlands). Plasma was separated from blood cells, 1 mL plasma was loaded onto a Sep-Pak tC18 cartridge (Waters, Etten-Leur, the Netherlands), and the cartridge was washed with 20 mL of water. This eluate was defined as the polar radiolabeled metabolite fraction. Next, the Sep-Pak cartridge was eluted with 1.5 mL of methanol. This eluate was defined as the non-polar fraction, and also contains the parent tracer. It was analyzed using HPLC (method G). The recovery from the Sep-pak procedure was >85% and rest activity was not taken into account. One half of the brain was counted for activity and the other half was homogenized with an ultrasonic homogenizer (Braunsonic 1510,

Table 1
Parent tracer and radiolabeled metabolite fractions in plasma (% of total radioactivity, mean ± SD; after intravenous injection of tracers under isoflurane anesthesia); for chemical structures, see Fig. 1.

	Min	[^{18}F]**1**	[^{18}F]**1** d_4	[^{18}F]**2**	[^{18}F]**2** d_4	[^{18}F]**3** d_3	[^{18}F]**3** d_7
Parent tracer	5	46 ± 14%	42 ± 12%	20 ± 3%	36 ± 6%	34 ± 5%	45 ± 3%
	15	19 ± 2%	23 ± 3%	8 ± 3%	15 ± 2%	18 ± 4%	24 ± 2%
	60	3 ± 1%	1 ± 0.3%	4 ± 1%	4 ± 1%	6 ± 1%	7 ± 1%
Non-polar metabolites	5	5 ± 2%	8 ± 4%	5 ± 3%	5 ± 6%	6 ± 1%	19 ± 3%
	15	9 ± 3%	9 ± 0.4%	5 ± 1%	4 ± 1%	7 ± 0.2%	23 ± 3%
	60	5 ± 0.5%	8 ± 1%	3 ± 1%	5 ± 1%	5 ± 1%	13 ± 1%
Polar metabolites	5	49 ± 11%	47 ± 7%	75 ± 3%	59 ± 4%	60 ± 5%	36 ± 5%
	15	71 ± 2%	68 ± 3%	87 ± 1%	81 ± 2%	75 ± 4%	52 ± 5%
	60	92 ± 1%	92 ± 1%	93 ± 2%	91 ± 1%	89 ± 2%	80 ± 3%

Germany) in cold water/MeCN (1:1, %v/v), under ice cooling, and subsequently centrifuged at 4000 rpm for 5 min. Separated supernatants were analyzed using HPLC.

Statistical analysis was performed using Graphpad PRISM (v 5.02, Graphpad Software Inc.). The metabolic stability (% parent tracer) of the deuterated tracers was compared to the non-deuterated analogs using a two-tailed unpaired *t*-test. Differences were considered significant if $p < 0.05$.

2.6. PET imaging and data analysis

Mice (25–32 g; *Mdr1a/b*$^{(-/-)}$ mice: $n = 3$; WT mice: $n = 4$) were anesthetized via a nose mask using 2% isoflurane in oxygen at a rate of 1 L·min^{-1}. One hour prior to each study, a jugular vein was cannulated for administration of the tracer. Animals were scanned on small animal NanoPET/CT or NanoPET/MR scanners (Mediso Ltd., Budapest, Hungary) [24] with identical PET components. The CT was used for attenuation correction and the MR scan for co-registration purposes. Next, a dynamic emission scan of 60 min was acquired immediately following administration of 3.77 ± 0.58 MBq of [^{18}F]**3-d_7**. Dynamic scans were acquired in list mode and rebinned into the following frame sequence: 4 × 5 s, 4 × 10 s, 2 × 30 s, 3 × 60 s, 2 × 300 s, 3 × 600 s, 1 × 900 s.

Reconstruction of nanoPET emission scans was performed using an iterative 3D Poisson ordered-subsets expectation-maximization algorithm (Tera-Tomo; Mediso Ltd. [24]) with 4 iterations and 6 subsets, resulting in an isotropic 0.4 mm voxel dimension. The reported spatial resolution of the scanners is 1 mm^2. PET images were analyzed using the freely available AMIDE software (version 0.9.2) [25]. Ellipsoidal shaped whole brain ROIs were drawn manually, based on anatomical structure indicated by the MR or CT scan. These ROIs were projected onto the dynamic image sequences, generating whole brain time-activity curves (TACs). All TACs were expressed as mean of standardized uptake values (SUV) within the VOI. SUV is a unitless parameter resulting from the normalization of the measured activity to injected dose and body weight.

3. Results & discussion

In a previous study, two fluorine-18 labeled verapamil analogs were evaluated, [^{18}F]**1** and [^{18}F]**2** [6]. Although *in vivo* results showed P-gp substrate behavior, metabolism of both tracers was increased compared with (*R*)-[^{11}C]verapamil. As rapid metabolism may compromise both signal to noise ratios and quantitative analysis, the purpose of the present study was to assess whether metabolic stability could be improved using deuterium substitution, an approach that has been successful for other tracers [18–21]. Four new analogs were synthesized and evaluated (Fig. 1). [^{18}F]**1-d_4** and [^{18}F]**2-d_4** were exact deuterium substituted analogs of [^{18}F]**1** and [^{18}F]**2**, with four deuterium atoms substituted on the fluoroethyl group. To gain more insight in the role of the original amine bound methyl group of verapamil, two other analogs of [^{18}F]**2** were synthesized, [^{18}F]**3-d_3** and [^{18}F]**3-d_7**, both with a deuterated methyl group. The difference between these two analogs was the (non-)deuterated fluoroethyl group.

3.1. Chemistry

The syntheses of the precursors and reference compounds were almost identical to those of the non-deuterated compounds, which have been described previously [6]. The use of commercially available deuterated starting materials ethylene-d_4 glycol and 2-bromoethanol-1,1,2,2-d_4 resulted in straightforward syntheses and ensured reliable isotopic purity.

Ethylene-d_4 glycol was di-tosylated with tosylchloride (Scheme 1) to be directly linked to the Boc-protected phenyl amine **8** (Scheme 2). The deprotected amine **10** was coupled to the (*R*)-aldehyde **15** as described previously [6] and it was directly protected with a Boc group to prevent formation of dimers, resulting in the precursor **17** of tracer [^{18}F]**2-d_4** (Scheme 3).

To synthesize the deuterated reference compound **18** of [^{18}F]**2-d_4** the tosyl group on the Boc protected amine **9** was fluorinated with TBAF to form amine **11**. After deprotection, amine **12** was coupled to aldehyde **15** by reductive amination, resulting in the reference compound **18**.

The two precursors **16** and **19** of [^{18}F]**3-d_3** and [^{18}F]**3-d_7**, respectively, were synthesized from aldehyde **15** and the (deuterated) amines **13** and **10**. After reductive amination, the secondary amine was methylated with Iodomethane-d_3 (Scheme 3). The two precursors **16** and **19** were both very difficult to purify and preparative HPLC was needed. Due to this extra step a lot of material was lost resulting in low yields. In future studies, this step needs to be optimized.

Table 2
Parent tracer and radiolabeled metabolite fractions in brain tissue (% of total radioactivity, mean ± SD; after intravenous injection of tracers under isoflurane anesthesia); for chemical structures, see Fig. 1.

	Min	[^{18}F]**1**	[^{18}F]**1** d_4	[^{18}F]**2**	[^{18}F]**2** d_4	[^{18}F]**3** d_3	[^{18}F]**3** d_7
Parent tracer	5	41 ± 10%	55 ± 6%	26 ± 6%	46 ± 4%	50 ± 6%	60 ± 6%
	15	14 ± 2%	27 ± 1%	17 ± 7%	34 ± 4%	26 ± 4%	38 ± 3%
	60	2 ± 0.3%	0.2 ± 0.1%	6 ± 1%	11 ± 2%	7 ± 0.2%	8 ± 2%
Brain metabolites	5	59 ± 10%	36 ± 24%	74 ± 6%	54 ± 4%	50 ± 6%	40 ± 6%
	15	86 ± 2%	73 ± 1%	83 ± 7%	64 ± 1%	74 ± 4%	62 ± 3%
	60	98 ± 0.3%	100 ± 0.1%	94 ± 1%	89 ± 2%	93 ± 0.2%	92 ± 2%

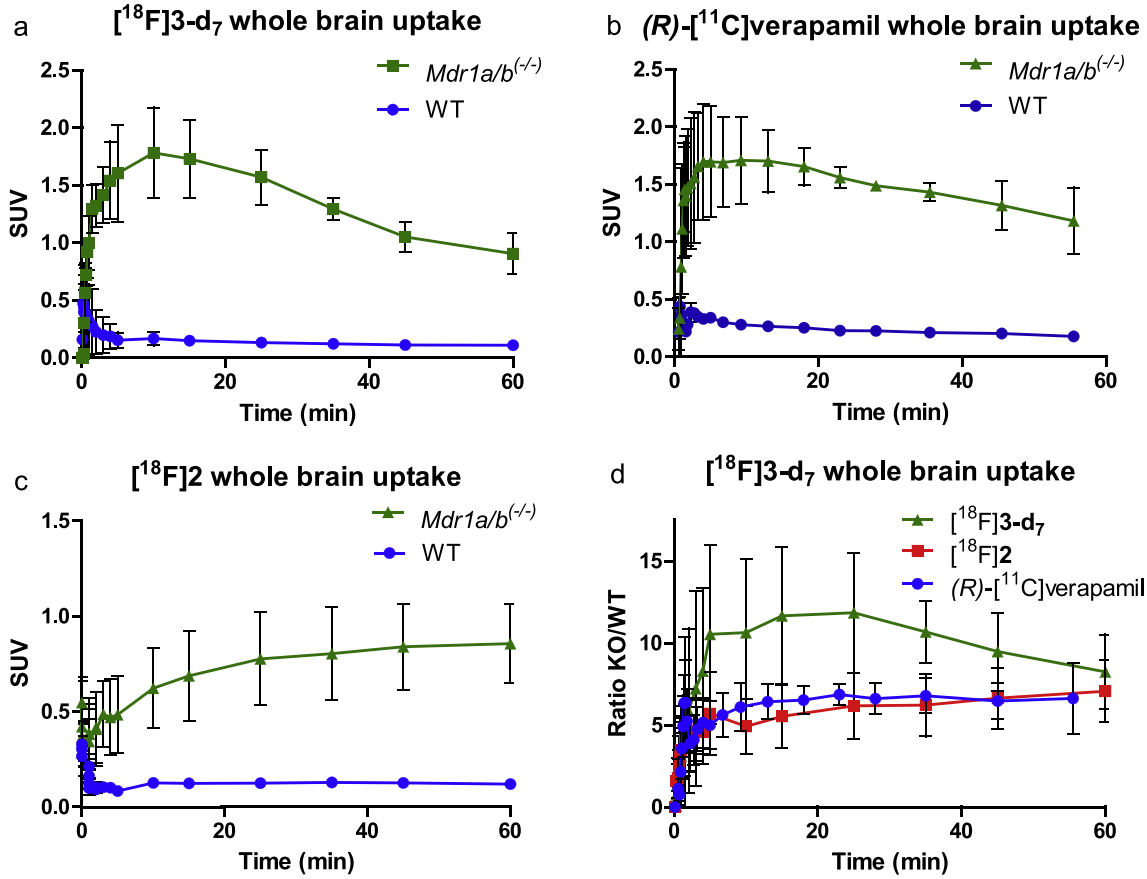

Fig. 3. Whole brain time-activity curves of a) [^{18}F]**3** ***d*$_7$**, b) (*R*) [^{11}C]verapamil and c) [^{18}F]**2** in ● wild-type (WT) mice and ■ *Mdr1a/b*$^{(-/-)}$ mice [6]. d) Ratio of *Mdr1a/b*$^{(-/-)}$ SUV over WT SUV with ▲[^{18}F]**3** ***d*$_7$**, ■ [^{18}F]**2** and ● (*R*) [^{11}C]verapamil. Mice were injected with 3–4 MBq of [^{18}F]**3** ***d*$_7$** under isoflurane anesthesia for 60 min.

For the reference compound of [^{18}F]**2-*d*$_4$**, the reference compound of [^{18}F]**2** was used [6] and methylated with Iodomethane-d_3.

Since the reference compound was used to identify the tracers by co-elution on analytical HPLC, the effect of deuterium substitution on elution time was tested. No difference in elution time between [^{18}F]**2** and [^{18}F]**2-*d*$_4$** was observed for different HPLC systems and therefore the reference compound of [^{18}F]**1** could be used for [^{18}F]**1-*d*$_4$** and the reference compound of [^{18}F]**3-*d*$_3$** for [^{18}F]**3-*d*$_7$**.

3.2. Radiochemistry

2-Bromoethanol-d_4 was tosylated (Scheme 1) and the purified oil was used as such to synthesize [^{18}F]**1-*d*$_4$** (Scheme 4). For [^{18}F]**1-*d*$_4$**, the same method was used as described before [6], where 2-bromoethyltosylate-d_4 was fluorinated and distilled to a second vial. On average 25% of [^{18}F]**21** was distilled to the second vial. The conversion of the second step to [^{18}F]**1-*d*$_4$**, varied from 5 to 27% and stirring was necessary to obtain product with a total yield of 2.64 ± 2.26% DC ($n = 7$). This resulted in enough product to perform animal experiments.

[^{18}F]**2-*d*$_4$** was radiolabeled as previously described [6], with direct fluorination and deprotection of the Boc group to result in a total yield of 6.10 ± 2.62% DC ($n = 3$) (Scheme 5).

[^{18}F]**3-*d*$_3$** and [^{18}F]**3-*d*$_7$** were radiolabeled in exactly the same manner, i.e. by direct fluorination on the tosyl group. Purification was challenging since traces of unlabeled fluorine were found in the product. To circumvent this, a purification step with an Alumina Sep-Pak was introduced to trap free and unreacted [^{18}F]fluorine on the Sep-Pak, before HPLC purification. This resulted in collected product with a radiochemical purity >99.5% and a total yield of 2.74 ± 0.71% DC (n = 3) and 4.90 ± 3.86% DC ($n = 5$) for [^{18}F]**3-*d*$_3$** for [^{18}F]**3-*d*$_7$**, respectively. As the precursors were not 99.9% pure, an additional radiochemical purity check was included using an HPLC system with a different column and eluent.

3.3. Metabolite study

Metabolite analyses of four novel tracers were performed in healthy Wistar rats, 5, 15 and 60 min after tracer injection. As the focus of the present study was on the comparison of stabilities of analog compounds, only male animals were used in order to avoid possible variation due to gender differences. In order to exclude possible differences in *in vivo* behavior of the tracers due to gender differences, a follow-up study should be performed for the most promising analog. This is beyond the scope of the present study. Statistical analysis of the metabolite data was performed using two-tailed unpaired *t*-tests. For plasma (Table 1), no improvement in metabolic stability was observed when moving from the hydrogenated to the deuterated [^{18}F]**1** tracer. On the other hand, for the [^{18}F]**2(-*d*$_4$)** analogs, an significant improvement in stability due to the deuterated fluoroethyl group was observed ($p < 0.05$, for 5 and 15 min). This could indicate that a different metabolic pathway for *N*-defluorethylation takes place, where the C—D bond is not included in the rate limiting step. Nonetheless, [^{18}F]**2-*d*$_4$** was less stable in plasma than non-deuterated [^{18}F]**1**. It seems that the tertiary amine slows down the metabolic rate, possibly by steric hindrance. To test this hypothesis, a deuterated methyl group on the amine was added in additional analogs, i.e. [^{18}F]**3-*d*$_3$** and [^{18}F]**3-*d*$_7$**, without and with the deuterated fluoroethyl group on the phenolic side.

The addition of a deuterated methyl group on the amine showed even higher *in vivo* stability. This actually contradicts the first assumption in the design of [^{18}F]**2** [6], which was based on the postulation that removal of the methyl group would circumvent the first metabolic step (demethylation). Nevertheless, adding a deuterated methyl group

Table 3
Log $D_{7.4}$ measurements.

Tracer	log $D_{7.4}$
[^{18}F]**1**	2.09
[^{18}F]**1** d_4	1.75
[^{18}F]**2**	1.61
[^{18}F]**2** d_4	1.45
[^{18}F]**3** d_3	2.16
[^{18}F]**3** d_7	2.19
[^{11}C]Verapamil [28]	2.66

on the amine still served the purpose of avoiding fluorine-18 labeled metabolites, which may also act as substrates of P-gp. For almost all tracers, primarily polar metabolites were formed, which are not expected to penetrate the BBB and therefore will not interfere with the PET signal. Interestingly, [^{18}F]**3-d_7** showed a different pattern with more labeled non-polar metabolites in plasma. This might reflect a metabolite that is formed after metabolic cleavage of the C—N bond on the stereoselective side of the molecule, with the deuterated methyl group still attached.

Brain tissue showed a different distribution between parent tracer and metabolites because some metabolites do not cross the blood-brain barrier. In the brain (Table 2), significantly more parent [^{18}F]**1-d_4** is present compared with [^{18}F]**1** ($p < 0.0005$ at 15 min). For [^{18}F]**2**, an increased parent fraction for the deuterated analog is even more prevalent ($p < 0.05$ at 5 and 15 min). Similar to the pattern in plasma, the combination of deuterated methyl and fluoroethyl groups ([^{18}F]**3-d_7**) results in the highest fraction of parent tracer, until the 60 min time point, when [^{18}F]**2-d_4** showed the highest parent fraction in the brain.

3.4. PET study

To assess *in vivo* behavior, a PET study was performed in control and *Mdr1a/b*$^{(-/-)}$ mice with the overall metabolically most stable tracer [^{18}F]**3-d_7** (Fig. 4). Increased brain uptake was observed in *Mdr1a/b*$^{(-/-)}$ mice compared with wild type mice (Fig. 3a). Washout was slow and similar to that of (*R*)-[^{11}C]verapamil in the brain (Fig. 3b). The ratio in whole brain uptake between *Mdr1a/b*$^{(-/-)}$ and wild type mice was significantly higher for [^{18}F]**3-d_7** than for [^{11}C]verapamil ($p = 0.0067$, paired *t*-test) (Fig. 3c). Data from the previous study [6] with the same PET experiments shows a different pattern for [^{18}F]**2**, where steady brain uptake was seen (although SUV remained below 1) without appreciable washout. This could be caused by the additional (deuterated) methyl group and consequently difference in log D (1.61 and 2.19 for [^{18}F]**2** and [^{18}F]**3-d_7**, respectively (Table 3)), suggesting that the methyl group affects in vivo behavior and (in this case) leads to increased brain penetration in *Mdr1a/b*$^{(-/-)}$ mice.

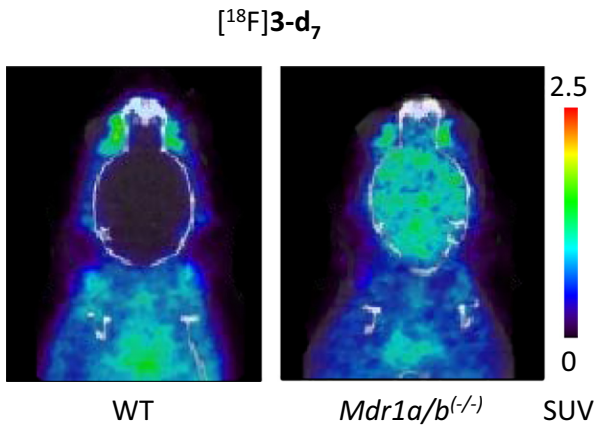

Fig. 4. Representative horizontal brain PET/CT images of [^{18}F]**3** d_7 in WT and *Mdr1a/b*$^{(-/-)}$ mice.

Related to the lipophilicity, plasma protein binding could be an important factor for successful clinical implementation of a PET tracer. (*R*)-[^{11}C]verapamil showed 88% plasma protein binding in human plasma [26], which did not limit its use for imaging. In general, high lipophilic PET tracers show high plasma protein binding [27]. Since all tracers developed are structurally similar to verapamil, but lower in lipophilicity (Table 3), no problems are expected with respect to plasma protein binding. To resolve the true value of the new PET tracer [^{18}F]**3-d_7**, clinical studies are needed. Possible study limitations for translation might be a different route of administration in the clinic, difference in metabolism between species and a laborious precursor syntheses route.

In the present study, no assessment of specificity toward P-gp in comparison with other transporters was performed. However, both (*R*)-[^{11}C]verapamil and [^{18}F]**2** are specific for P-gp, and this is also expected for the structurally similar analog [^{18}F]**3-d_7**.

4. Conclusion

The metabolic stability of existing fluorine-18 labeled verapamil analogs can be improved by inclusion of deuterium in the tracer molecule. In addition, increased metabolic stability of the methyl containing analogs [^{18}F]**3-d_3** and [^{18}F]**3-d_7** was observed, which may be the result of steric hindrance of enzymatic metabolism. The similarity of *in vivo* behavior between [^{18}F]**3-d_7** and (*R*)-[^{11}C]verapamil, together with improved metabolic stability of [^{18}F]**3-d_7**, compared to the other fluorine-18 labeled tracers, supports the potential of [^{18}F]**3-d_7** as a candidate for clinical translation as a fluorine-18 labeled PET tracer for evaluation of P-gp.

Acknowledgments

This study was funded by the Dutch Technology Foundation STW (project number 11741). Fluorine-18 was kindly provided by BV Cyclotron (Amsterdam, The Netherlands).

Conflicts of interest

The authors declare no conflict of interest.

Appendix A. Supplementary data

Supplementary data to this article can be found online at https://doi.org/10.1016/j.nucmedbio.2018.06.009.

References

[1] Schinkel AH. P-Glycoprotein, a gatekeeper in the blood–brain barrier. Adv Drug Deliv Rev 1999;36:179–94.
[2] van Assema DME, van Berckel BNM. Blood-brain barrier ABC-transporter P-glycoprotein in Alzheimer's disease: still a suspect? Curr Pharm Des 2016;22:5808–16.
[3] Lazarowski A, Czornyj L, Lubienieki F, Girardi E, Vazquez S, D'Giano C. ABC transporters during epilepsy and mechanisms underlying multidrug resistance in refractory epilepsy. Epilepsia 2007;48(Suppl. 5):140–9.
[4] Luurtsema G, Elsinga PH, Dierckx RA, Boellaard R, van Waarde A. PET tracers for imaging of ABC transporters at the blood-brain barrier: principles and strategies. Curr Pharm Des 2016;22:5779–85.
[5] Vohra J. Verapamil in cardiac arrhythmias: an overview. Clin Exp Pharmacol Physiol Suppl 1982;6:129–34.
[6] Raaphorst RM, Luurtsema G, Schuit RC, Kooijman EJM, Elsinga PH, Lammertsma AA, et al. Synthesis and evaluation of new fluorine-18 labeled verapamil analogs to investigate the function of P-glycoprotein in the blood-brain barrier. ACS Chem Nerosci 2017;8:1925–36.
[7] Pauli-Magnus C, von Richter O, Burk O, Ziegler A, Mettang T, Eichelbaum M, et al. Characterization of the major metabolites of verapamil as substrates and inhibitors of P-glycoprotein. J Pharmacol Exp Ther 2000;293:376–82.
[8] von Richter O, Eichelbaum M, Schonberger F, Hofmann U. Rapid and highly sensitive method for the determination of verapamil, [$^2H_7$]verapamil and metabolites in biological fluids by liquid chromatography-mass spectrometry. J Chromatogr B 2000;738:137–47.

[9] Kroemer HK, Gautier J-C, Beaune P, Henderson C, Wolf CR, Eichelbaum M. Identification of P450 enzymes involved in metabolism of verapamil in humans. Naunyn Schmiedebergs Arch Pharmacol 1993;348:332–7.
[10] Busse D, Cosme J, Beaune P, Kromer HK, Eichelbaum M. Cytochromes of the P450 2C subfamily are the major enzymes involved in the O-demethylation of verapamil in humans. Naunyn Schmiedebergs Arch Pharmacol 1995;353:116–21.
[11] Luurtsema G, Molthoff CF, Schuit RC, Windhorst AD, Lammertsma AA, Franssen EJ. Evaluation of (R)-[11C]verapamil as PET tracer of P-glycoprotein function in the blood-brain barrier: kinetics and metabolism in the rat. Nucl Med Biol 2005;32:87–93.
[12] Meyer AH, Dybala-Defratyka A, Alaimo PJ, Geronimo I, Sanchez AD, Cramer CJ, et al. Cytochrome P450-catalyzed dealkylation of atrazine by *Rhodococcus* sp. strain NI86/21 involves hydrogen atom transfer rather than single electron transfer. Dalton Trans 2014;43:12175–86.
[13] Wiberg KB. The deuterium isotope effect. Chem Rev 1955;55:713–43.
[14] Westheimer FH. The magnitude of the primary kinetic isotope effect for compounds of hydrogen and deuterium. Chem Rev 1961;61:265–73.
[15] Harbeson SL, Tung RD. Deuterium medicinal chemistry: a new approach to drug discovery and development. MedChem News 2014:8–22.
[16] Mullard A. Deuterated drugs draw heavier backing. Nat Rev Drug Discov 2016;15:219–21.
[17] FDA (U.S. Food and Drug Administration). New drug application approval 208082 reference ID: 4078379. Available at https://www.accessdata.fda.gov/scripts/cder/daf/index.cfm; 2017, Accessed date: 28 May 2018. [under Austedo (deutetrabenazine)].
[18] Fowler JS, Wang G-J, Logan J, Xie S, Volkow ND, MacGregor RR, et al. Selective reduction of radiotracer trapping by deuterium substitution: comparison of carbon-11-L-deprenyl and carbon-11-deprenyl-D2 for MAO B mapping. J Nucl Med 1995;36:1255–62.
[19] Smith G, Zhao Y, Leyton J, Shan B, Nguyen QD, Perumal M, et al. Radiosynthesis and preclinical evaluation of [(18)F]fluoro-[1,2-(2)H(4)]choline. Nucl Med Biol 2011;38:39–51.
[20] Witney TH, Alam IS, Turton DR, Smith G, Carroll L, Brickute D, et al. Evaluation of deuterated 18F- and 11C-labeled choline analogs for cancer detection by positron emission tomography. Clin Cancer Res 2012;18:1063–72.
[21] van Dyck CH, Soares JC, Tan P-Z, Staley JK, Baldwin RM, Amici LA, et al. Equilibrium modeling of 5-HT_{2A} receptors with [^{18}F]deuteroaltanserin and PET: feasibility of a constant infusion paradigm. Nucl Med Biol 2000;27:715–22.
[22] Windhorst AD, ter Linden T, de Nooij A, Keus JF, Buijs FL, Schollema PE, et al. A complete, multipurpose, low cost, fully automated and GMP compliant radiosynthesis system. J Label Compd Radiopharm 2001;44:S1052–4.
[23] Klein PJ, Chomet M, Metaxas A, Christiaans JA, Kooijman E, Schuit RC, et al. Synthesis, radiolabeling and evaluation of novel amine guanidine derivatives as potential positron emission tomography tracers for the ion channel of the N-methyl-D-aspartate receptor. Eur J Med Chem 2016;118:143–60.
[24] Szanda I, Mackewn J, Patay G, Major P, Sunassee K, Mullen GE, et al. National Electrical Manufacturers Association NU-4 performance evaluation of the PET component of the NanoPET/CT preclinical PET/CT scanner. J Nucl Med 2011;52:1741–7.
[25] Loening AM, Gambhir SS. AMIDE: a free software tool for multimodality medical image analysis. Mol Imaging 2003;2:131–7.
[26] Sasongko L, Link JM, Muzi M, Mankoff DA, Yang X, Collier AC, et al. Imaging P-glycoprotein transport activity at the human blood-brain barrier with positron emission tomography. Clin Pharmacol Ther 2005;77:503–14.
[27] Zoghbi SS, Anderson KB, Jenko KJ, Luckenbaugh DA, Innis RB, Pike VW. On quantitative relationships between drug-like compound lipophilicity and plasma free fraction in monkey and human. J Pharm Sci 2012;101:1028–39.
[28] Zhu C, Jiang L, Chen T-M, Hwang K-K. A comparative study of artificial membrane permeability assay for high throughput profiling of drug absorption potential. Eur J Med Chem 2002;37:399–407.